

Microsporidium goeldichironomi n. sp. and *Microsporidium chironomi* n. sp. (Microsporida: Apansporoblastina): Two New Microsporidia from Florida Chironomids¹

JOHN KNELL²

Department of Entomology and Nematology, University of Florida, Gainesville, Florida 32611

Received November 21, 1978

Two new species of Microsporida belonging to the genus *Microsporidium* are described. *Microsporidium goeldichironomi* n. sp. parasitizes the fat body of *Goeldichironomus holoprasinus* and *Microsporidium chironomi* n. sp. infects *Chironomus attenuatus*. Both microsporidia form uninucleate spores from rosette-shaped sporonts. *M. goeldichironomi* sporonts form 4, 6, 8, 10, 12, 16, and possibly more spores. Two shapes of spores are produced, oval, or slightly pyriform spores measuring $3.70 \pm 0.09 \times 2.49 \pm 0.13 \mu\text{m}$ and pyriform spores measuring $3.74 \pm 0.44 \times 2.04 \pm 0.17 \mu\text{m}$. Electron micrographs show that both types of spores are uninucleate, have 8 to 11 polar filament coils and a lamellate polaroplast showing several distinct regions. *M. chironomi* spores are pyriform and are often joined at the posterior end in groups of two or four. They measure $4.12 \pm 0.37 \times 2.45 \pm 0.26 \mu\text{m}$. The spores are uninucleate, have six to seven polar filament coils and a lamellate polaroplast showing two distinct regions. Neither species can be transmitted per os and thus are assumed to be transovarially transmitted. No pansporoblastic membrane is present in either species.

KEY WORDS: *Microsporidium goeldichironomi*; *Microsporidium chironomi*.

INTRODUCTION

During the winter and spring of 1973 a number of moribund chironomid larvae were recovered from aeration ponds of the University of Florida sewage treatment plant. The chironomids were identified as *Chironomus attenuatus* and *Goeldichironomus holoprasinus* and were white in color as opposed to the red color of healthy larvae. Microscopical examination showed that the chironomids were infected with two distinct species of Microsporida which are described in the following report.

MATERIALS AND METHODS

Field-collected chironomids were examined in a black plastic pan to detect patently infected larvae. The heads and last few abdominal segments of infected specimens were cut off and preserved in 70% ethanol prior to mounting in CMC-10 aqueous

medium for identification of the chironomids. The remainder of the body was cut into small segments to be used for examination of fresh spores by employing Giemsa smears, Heidenhain smears, and electron microscopy. Photographs and measurements were made of spores immersed in immersion oil to mitigate Brownian movement. Measurements were made using an A.E.I. Cook image-splitting micrometer at 1000 \times .

Giemsa smears were prepared by smearing the tissue on microscope slides, air drying, fixing in 95% methanol for 5 min, staining with a 10% Giemsa solution made with sodium phosphate buffer, pH 7.41 (Fisher Gram-Pac), for 10 min, and washing in tap water. Heidenhain smears were prepared by smearing infected tissue on glass coverslips, fixing for at least 6 hr in aqueous Bouin's, washing in 70% ethanol, staining in Heidenhain's hematoxylin, and mounting on microscope slides.

For paraffin sectioning, larvae were fixed for 2–4 hr in Carnoy's solution, rinsed for 1

¹ University of Florida Journal Series No. 1528.

² Present address: Department of Entomology, Texas A & M University, College Station, Tex. 77843.

hr in 70% ethanol, then left in 70% ethanol overnight. Dehydration was accomplished by immersion in a graded series of ethanol. The tissue was cleared in three 2-hr washes in 100% butanol and embedded in Tissuemat. Sections were cut at 6–8 μm on a rotary microtome and stained with Heidenhain's hematoxylin and eosin.

For electron microscopy, small pieces of tissue were fixed overnight in 4% gluteraldehyde in 0.1 M sodium cacodylate buffer, pH 7.2, maintained at 4–8°C. After fixation, the tissue was washed twice in 0.1 M cacodylate buffer, then maintained in buffer overnight. Postfixation was accomplished in 1% OsO₄ in 0.1 M cacodylate buffer for 2 hr at room temperature, after which the tissue was dehydrated by passage through increasing concentrations of ethanol to propylene oxide, and embedded in Epon–araldite (Mollenhauer, 1964). Gold sections were picked up on carbon-stabilized formvar-coated 300-mesh copper grids and stained with uranyl acetate and lead citrate (Venable and Coggeshall, 1965). The sections were examined and photographed with an Hitachi 125-E electron microscope,

using an accelerating voltage of 50 kV. Polar filament angles of tilt were measured according to Burges et al. (1974).

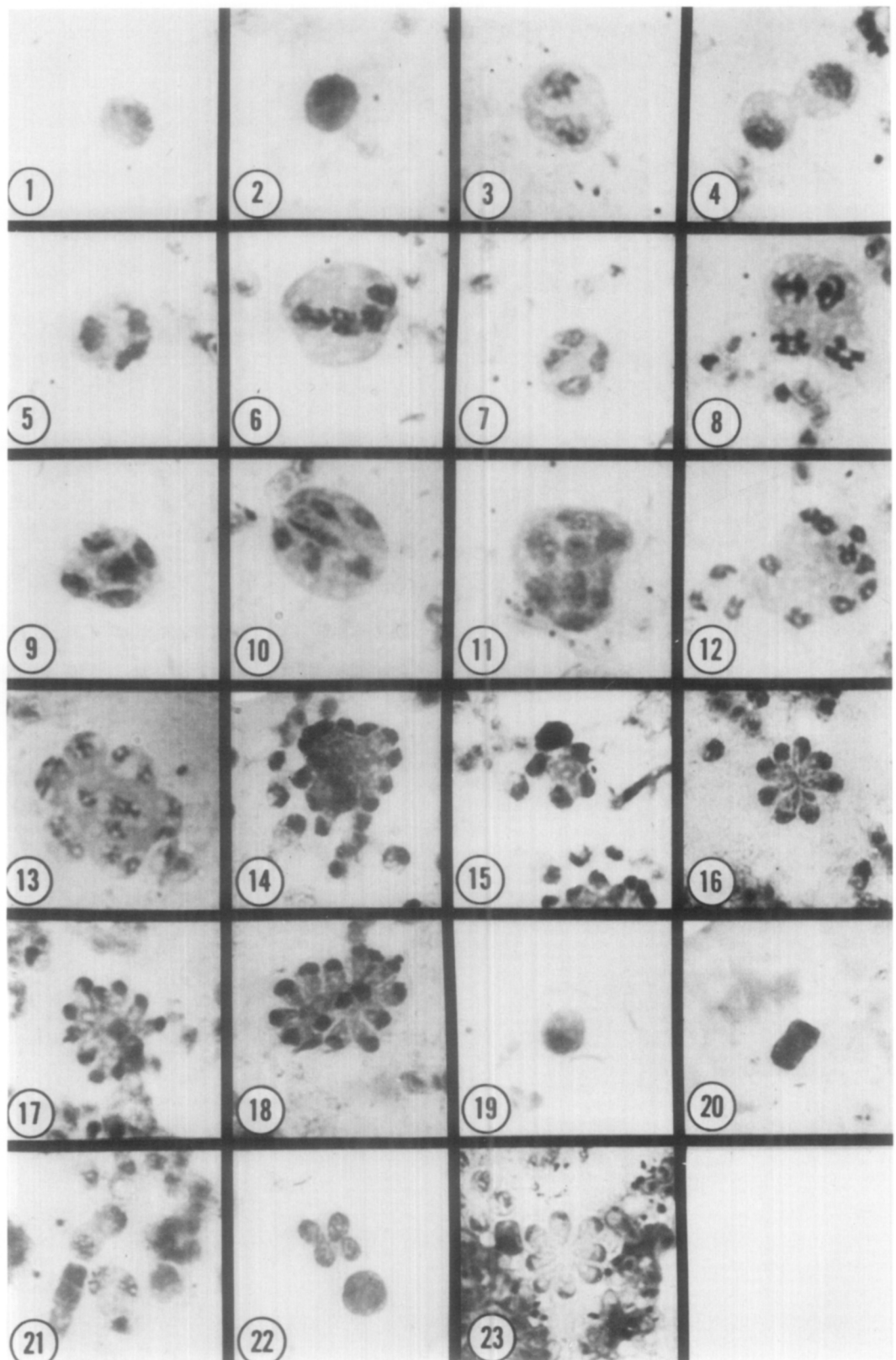
RESULTS

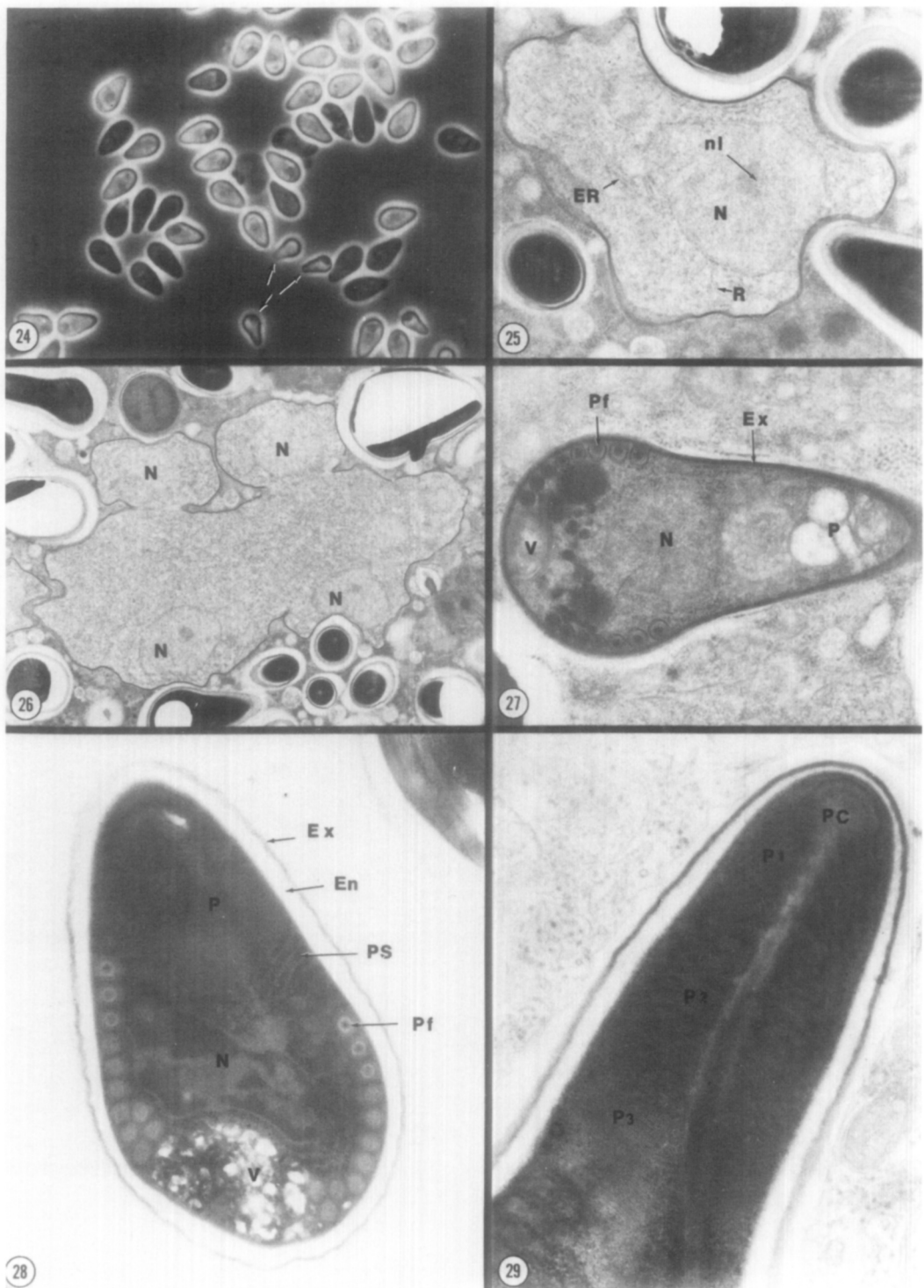
Microsporidium goeldichironomi n. sp.

This microsporidium was originally found infecting fourth-instar larvae of the chironomid midge *G. holoprasinus* in the aeration ponds of the University of Florida sewage treatment plant. Subsequently, it has also been recovered from the greenhouse operated by the Insect Attractants Laboratory, U.S. Department of Agriculture, and from some ponds used for insecticide testing by the Insects Affecting Man Laboratory, U.S. Department of Agriculture. The parasite infects the posterior half of the abdomen of the larva, turning it a bright white which contrasts with the normal red color of the uninfected anterior region. Paraffin sections show that the only organ invaded is the fat body, which is completely packed with spores. To date all attempts to infect larvae per os have failed. This fact plus the very low prevalence of infection (less than 1%) indicates that *M.*

FIGS. 1–18. *Microsporidium goeldichironomi*.

- FIG. 1. Mononucleate vegetative state. Giemsa stain. 1540 \times .
- FIG. 2. Binucleate vegetative stage. Giemsa stain. 1540 \times .
- FIG. 3. Binucleate vegetative stage. Giemsa stain. 1540 \times .
- FIG. 4. Binucleate vegetative stage. Giemsa stain. 1540 \times .
- FIG. 5. Trinucleate vegetative stage. Giemsa stain. 1540 \times .
- FIG. 6. Tetranucleate vegetative stage. Giemsa stain. 1540 \times .
- FIG. 7. Tetranucleate vegetative stage. Giemsa stain. 1540 \times .
- FIG. 8. Tetranucleate vegetative stage. Giemsa stain. 1540 \times .
- FIG. 9. Pentanucleate vegetative stage. Giemsa stain. 1540 \times .
- FIG. 10. Hexanucleate vegetative stage. Giemsa stain. 1540 \times .
- FIG. 11. Octonucleate vegetative stage. Giemsa stain. 1540 \times .
- FIG. 12. Vegetative stage with 12 nuclei. Giemsa stain. 1540 \times .
- FIG. 13. Vegetative stage with 16 nuclei. Giemsa stain. 1540 \times .
- FIG. 14. Vegetative stage with 12 nuclei at periphery of cell. Giemsa stain. 1540 \times .
- FIG. 15. Budding sporont with four nuclei. Giemsa stain. 1540 \times .
- FIG. 16. Budding sporont with eight nuclei. Giemsa stain. 1540 \times .
- FIG. 17. Budding sporont with 12 nuclei. Giemsa stain. 1540 \times .
- FIG. 18. Budding sporont with 16 nuclei. Giemsa stain. 1540 \times .
- FIGS. 19–23. *Microsporidium chironomi*.
- FIG. 19. Mononucleate vegetative stage. Giemsa stain. 1540 \times .
- FIG. 20. Binucleate vegetative stage dividing. Giemsa stain. 1540 \times .
- FIG. 21. Tetranucleate vegetative stage dividing. Giemsa stain. 1540 \times .
- FIG. 22. Budding sporont with four nuclei. Giemsa stain. 1540 \times .
- FIG. 23. Budding sporont with eight nuclei. Giemsa stain. 1540 \times .





Figs. 24-29. *Microsporidium goeldichironomi*.

FIG. 24. Spores. Phase contrast. $1540\times$.

FIG. 25. Uninucleate vegetative stage. Electron micrograph. N, Nucleus; nl, endoplasmic reticulum; R, ribosomes. $12,035\times$.

goeldichironomi may be transmitted transovarially or may require an alternate host.

Light microscopy. Generally, few vegetative stages remain in patently infected larvae. The most common of these are uni- and binucleate cells having deep blue staining cytoplasm (Figs. 1–3). It is not unusual to find the binucleate forms in the act of cytokinesis (Fig. 4). Also present are larger cells possessing 3, 4, 6, 8, 10, 12, or 16 nuclei randomly scattered through the cytoplasm (Figs. 5–13). The nuclei of these cells often appear to be dividing (Figs. 8, 12–13).

The nuclei eventually migrate to the periphery of the cell (Figs. 12–14), then continue their outward migration pulling with them a coating of cytoplasm producing fingerlike projections (Figs. 15–18). Ultimately, these rosettes split apart giving rise to 4, 6, 8, 10, 12, or 16 spores.

The spores of this microsporidium are pyriform, white, and have a prominent vacuole at the posterior end (Fig. 24). Two different spores are produced. By far the most prevalent is a white pyriform spore measuring $3.70 \pm 0.09 \times 2.49 \pm 0.13 \mu\text{m}$ with a range of $3.55–3.87 \times 2.39–2.76 \mu\text{m}$. Occasionally present is a more sharply pointed pyriform spore which usually occurs mixed with the larger forms (Fig. 24, arrow) and occasionally is the dominant type. This spore measures $3.74 \pm 0.44 \times 2.04 \pm 0.17 \mu\text{m}$ with a range of $3.29–4.77 \times 1.86–2.49 \mu\text{m}$.

The polar filaments of this species extrude only when enough force is applied to crush the spore, and thus do not lend themselves to measurement.

Electron microscopy. The most common vegetative stage seen in sections are uninucleate cells which probably correspond to

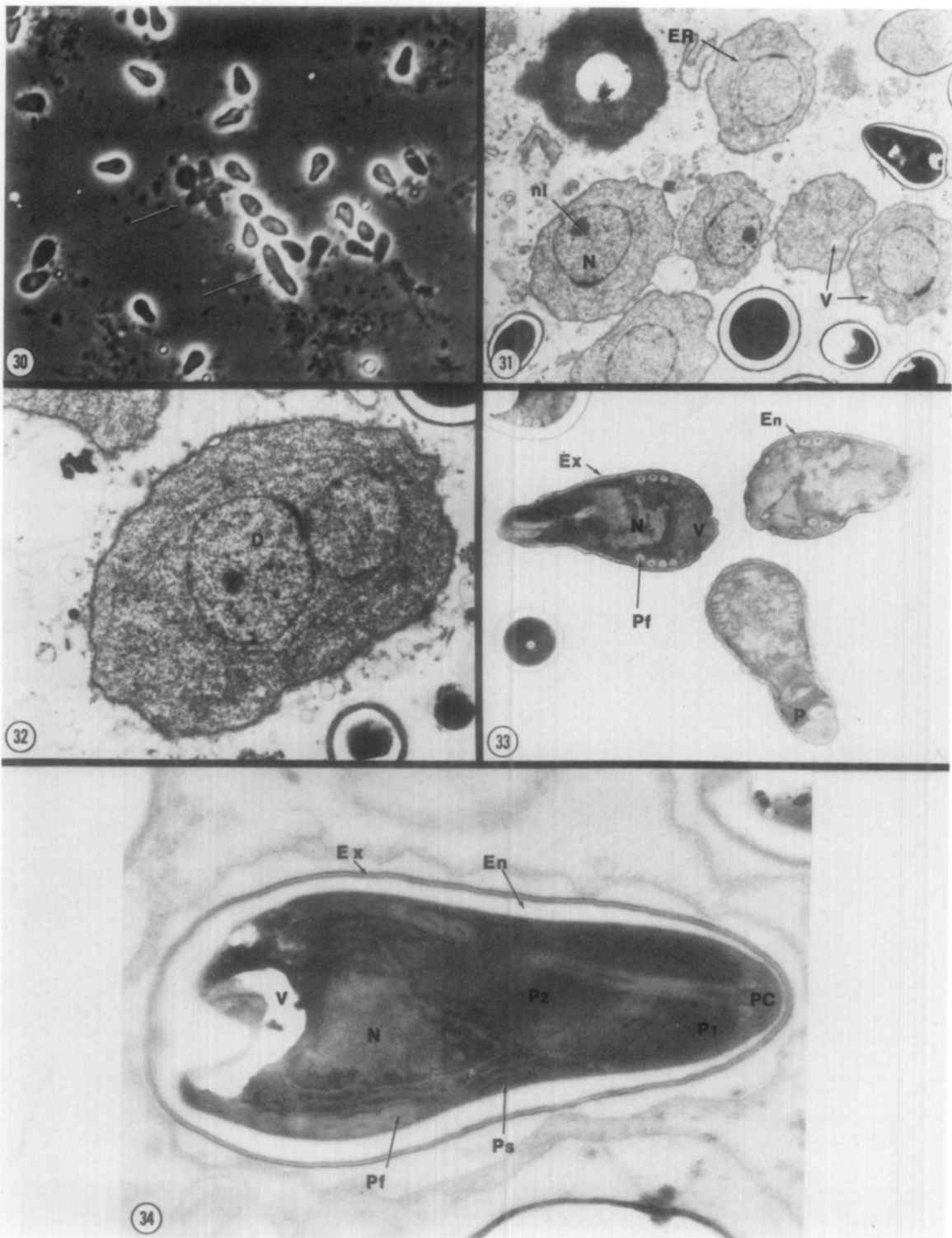
those seen in Figure 1. Besides the nucleus, which often contains a prominent nucleolus (Fig. 25, nl), the only organelle present is rough endoplasmic reticulum (Fig. 25, ER), and ribosomes (Fig. 25, R). It is also possible to find multinucleate plasmodia (sporonts), some of which are in the process of budding to form sporoblasts (Fig. 26). Later sporoblasts may be distinguished by the lack of the electron lucent endospore layer in the spore wall. At this stage only the electron dense exospore layer is formed (Fig. 27, Ex). Sporoblasts show the organelles of the mature spore in various stages of development such as the polar filament (Fig. 27, Pf), polaroplast (Fig. 27, P), nucleus (Fig. 27, N), and vacuole (Fig. 27, V). The two types of mature spores have similar ultrastructures. The spore wall is composed of an outer exospore (Fig. 28, Ex) and an inner endospore (Fig. 28, En). There is a single nucleus (Fig. 28, N) which contains electron dense areas located along its periphery. The polar filament has 8–11 coils (Fig. 28, Pf), with an angle of tilt of 57° for the anterior coil and 55° for the posterior. The nucleus is bordered by one to several rows of rough ER. It is separated from the polaroplast (Fig. 28, P) by up to five rows of rough ER (Fig. 28, Ps). The vacuole is located eccentrically in the posterior end of the spore (Fig. 28, V) and characteristically shows many electron lucent areas which are probably artifacts. The polaroplast fills the anterior portion of the spore (Figs. 28, 29, P). It is composed of a series of lamellae which abruptly become tightly compressed posteriorly. In the anterior third of the polaroplast the lamellae are oriented at an angle of approximately 45° with respect to the polar filament (Fig. 29, P1). In the middle third, the lamellae are

FIG. 26. Budding multinucleate sporont Electron micrograph. N, Nucleus. $5200\times$.

FIG. 27. Sporoblast. Electron micrograph. Ex, Exospore layer of spore wall; Pf, polar filament; N, nucleus; P, polaroplast; V, vacuole. $15,656\times$.

FIG. 28. Mature spore. Electron micrograph. En, Endospore; Ex, exospore; N, nucleus; Pf, polar filament; P, polaroplast; Ps, polysomes; V, vacuole. $14,040\times$.

FIG. 29. Polaroplast of *M. goeldichironomi*. Electron micrograph. P1, anterior region; P2, middle region; P3 posterior region; PC, polar cap. $32,448\times$.



Figs. 30-34. *Microsporidium chironomi*.

FIG. 30. Spores. Phase contrast. Arrows point to aberrant forms characteristic of the species. 941 \times .

perpendicular to the polar filament (Fig. 29, P2). Those in the posterior region are also perpendicular and are tightly compressed (Fig. 29, P3). The polar cap is located apically (Fig. 29, PC).

Microsporidium chironomi n. sp.

This microsporidium was found infecting larvae of *C. attenuatus* from the aeration ponds of the University of Florida sewage treatment plant. Frank infections appear in fourth-instar larvae as segmentally arranged, dull white bands throughout the entire body. Field-collected infected larvae are lethargic and generally die before pupating. The primary site of infection of *M. chironomi* is the fat body, although spores occasionally appear in the basal region of the cells of the proventriculus. As with *M. geoldichironomi*, all attempts to reinfect newly hatched larvae by feeding spores have failed. The infection rate of this microsporidian usually averages 7%.

Light microscopy. No schizogonic stages have been positively identified for this microsporidium. The most prevalent sporogonic stages are uni- (Fig. 19) and binucleate (Fig. 20) cells having dark blue staining cytoplasm and measuring 5 μm in diameter. The binucleate forms are often seen dividing (Fig. 20). Tetranucleate forms are also common and often have ring-shaped nuclei (Fig. 21). Typically these nuclei migrate to the periphery of the cell and bud off forming four sporoblasts (Fig. 22). Often the four nuclei divide once again before reaching the cell membrane producing eight sporoblasts (Fig. 23).

The spores are pyriform, white, have a large dark vacuole at the posterior end, and

measure $4.12 \pm 0.37 \times 2.45 \pm 0.26 \mu\text{m}$ with a range of $3.76-4.61 \times 2.01-2.76 \mu\text{m}$ (Fig. 24). Some oval spores may also be present but a more distinctive feature is the presence of aberrant forms. Two, three, four, or more pyriform spores may remain fused at the posterior end thus forming the star shape seen in Figure 30 (arrow). Less common are elongate or crescent shapes (Fig. 30, arrow).

Electron microscopy. The most frequently seen vegetative stages are uninucleate cells which probably correspond to those seen in Figure 19. The cells have a nucleus containing a prominent nucleolus (Fig. 31, nl) and often there is osmophilic material along the nuclear membrane. There is also rough ER (Fig. 31, ER) and some cells have small vacuoles (Fig. 31, V). Rarely, these sporonts have what may be a diplokaryon (Fig. 32, D). Sporoblasts may be differentiated from mature spores by the absence or incomplete development of the electron lucent endospore layer of the spore wall (Fig. 33, En). Sporoblasts contain the organelles of the mature spore in various stages of development. Those shown in Figure 33 show most of the polar filament coils (Pf), the nucleus (N), vacuole (V), polaroplast (P), exospore spore wall layer (Ex), and partially developed endospore layer (En). Mature spores have a thick endospore layer (Fig. 34, En) and thus, show the true shape of the spore in the sagittal sections. The exospore layer is composed of two electron dense layers with an electron lucent layer in between (Fig. 34, Ex). There are six to seven polar filament coils having an angle of tilt of 69° for the anterior coils and 60° for the posterior. There is a

FIG. 31. Uninucleate vegetative stages. Electron micrograph. N, Nucleus; nl, nucleolus; ER, endoplasmic reticulum; V, vacuole. 7734 \times .

FIG. 32. Vegetative stage containing a diplokaryon. Electron micrograph. D, Diplokaryon. 11,397 \times .

FIG. 33. Sporoblasts. Electron micrograph. En, Endospore layer; Ex, exospore layer; Pf, polar filament; N, nucleus; V, vacuole; P, polaroplast. 12,956 \times .

FIG. 34. Mature spore. Electron micrograph. En, Endospore layer; Ex, exospore layer; N, nucleus; Ps, polysomes; V, vacuole; P, polaroplast; PC, polar cap; P1, anterior region of polaroplast; P2, posterior region of polaroplast. 29,835 \times .

single nucleus, the periphery of which shows electron dense material (Fig. 34, N). The nucleus is bordered by approximately two rows of rough ER (Fig. 34, Ps). The vacuole is located eccentrically in the posterior of the spore and shows varying degrees of fixation artifacts (Fig. 34, V). The polaroplast occupies the anterior portion of the spore and is composed of two regions. There is an anterior portion composed of wide lamellae which are orientated at an angle of approximately 45° to the polar filament (Fig. 34, P₁) and a posterior region composed of tightly compressed lamellae (Fig. 34, P₂). The polar cap in this microsporidium is located apically (Fig. 34, PC).

DISCUSSION

The taxonomic position of these two microsporidia is not clear at this time. The sporulation sequence is similar to that of *Stempellia magna* (Kudo, 1920) and the "thin-walled spore" sequence of *Stempellia milleri* (Hazard and Fukuda, 1974). Recently, however, the type species of the genus *Stempellia*, *S. mutabilis* (Léger and Hesse, 1910) has been rediscovered and has been found to be quite different from *S. magna* and *S. milleri* (see Desportes, 1976). *S. mutabilis* produces groups of four and eight spores contained within a pansporoblastic membrane. This occurs in the fat body of *Emphemera vulgata* and causes the formation of a xenoma. Since neither *S. magna* nor *S. milleri* have a pansporoblastic membrane they have been assigned to the collective genus *Microsporidium* along with all other species except for the type, *S. mutabilis* (see Sprague, 1977). Due to their similarity to *S. magna* and *S. milleri*, the two microsporidia described above have been included in the collective genus *Microsporidium*.

Both *M. chironomi* and *M. goeldichironomi* may be differentiated from *S. magna* on the basis of spore size as *S. magna* is one of the largest microsporidia known having spores measuring 11.67 × 4.57 µm. The ultrastructure of the spore of *S. magna*

is also readily distinguished by the presence of a highly vacuolated polaroplast (Hazard and Fukuda, 1974). *S. milleri* may be distinguished on the basis of its sequence producing binucleate spores and by the fact it may be transmitted to its host *per os*. This is not possible with *S. magna* and the two *Microsporidium* spp. from chironomids. The spores of *S. milleri* are also larger than those of the two *Microsporidium* spp. measuring 4.91 × 2.50 µm.

Of the 16 species of microsporidians infecting chironomids listed by Weiser (1961), *Thelohania breindli* Weiser, 1946, *T. pinguis* Hesse, 1903, *T. hessei* Léger and Hesse, 1921, *T. chironomi* Jirovec, 1940, *Stempellia polyspora* Léger and Hesse, 1921, *Plistophora jiroveci* Weiser, 1942, and *P. chironomi* Debaisieux, 1931, may be distinguished from the two new species of *Microsporidium* as they all possess a pansporoblast membrane. This is also true for the *Gurleya* sp. infecting *Chironomus californicus* (see Hunter, 1968). *Bacillidium bacilliforme* Léger and Hesse, 1922, *B. tetrasporum* Léger and Hesse, 1916, and *Mrazekia brevicauda* Léger and Hesse, 1916, all have characteristic elongate spores while those of *Nosema micrococcus* Léger and Hesse, 1921, are spherical and those of *Toxoglugea chironomi* Debaisieux, 1931, are crescent shaped. In addition, ultrastructural studies have shown that the genus *Mrazekia* (including *Bacillidium*) has a pansporoblastic membrane (unpubl.). *Nosema zavreli* Weiser, 1946, infects the midgut of the larvae of *Chironomus thumi* whereas the two new species of *Microsporidium* infect only the fat body. Similarly, *N. chironomi* Lutz and Splendore, 1908, infects the posterior midgut of its host. *Octosporea chironomi* Weiser, 1943, has stages and spores with diplokarya while those of the two new species of *Microsporidium* are uninucleate.

M. chironomi and *M. goeldichironomi* may be differentiated on the basis of spore size and on the sporulation sequence. *M. chironomi* sporonts give rise to either four

or eight spores (Figs. 19–23) while those of *M. goeldichironomi* produce 4, 6, 8, 10, 12, 16, or more (Figs. 1–18). Ultrastructurally, they also differ, with *M. chironomi* having 6–7 polar filament coils and *M. goeldichironomi* having 8–11.

Both of the microsporidia described above are assumed to be transovarially transmitted. All attempts to transmit the pathogens by feeding newly hatched larvae on infected cadavers have failed. In addition, both pathogens are present in low densities. The entire substratum of the sewage treatment plant is composed of *Chironomus* and *Goeldichironomus* tubes. A pathogen capable of per os transmission would probably be present in much higher concentrations in such a habitat.

Giemsa smears, Heidenhain wet mounts, and electron microscope blocks of the type material will be deposited in the type collection of the National Museum in Washington, D.C.

ACKNOWLEDGMENTS

The author wishes to thank Mr. William C. Beck for his help in chironomid identification. I also thank Mrs. Susan Avery for her help preparing specimens for

electron microscopy and Mr. Edwin I. Hazard for his advice on microsporidian taxonomy.

REFERENCES

- BURGES, H. D., CANNING, E. U., AND HULLS, I. K. 1974. Ultrastructure of *Nosema oryzaephili* and the taxonomic value of the polar filament. *J. Invertebr. Pathol.*, 23, 135–139.
- DESPORTES, I. 1976. Ultrastructure de *Stempellia mutabilis* Léger et Hesse, microsporidie parasite de L'Empemere *Emphera vulgata* L. *Protistologica*, 12, 121–150.
- HAZARD, E. I., AND FUKADA, T. 1974. *Stempellia milleri* sp. n. (Microsporidia: Nosematidae) in the mosquito *Culex pipiens quinquefasciatus* Say. *J. Protozool.*, 21, 497–504.
- HUNTER, D. K. 1968. Response of populations of *Chironomus californicus* to a Microsporidian (*Gurleya* sp.). *J. Invertebr. Pathol.*, 10, 387–389.
- KUDO, R. 1920. Cnidosporida in the vicinity of Urbana. *Trans. Ill. St. Acad. Sci.*, 13, 298–303.
- LÉGER, L., AND HESSE, E. 1910. Cnidosporidies des larves d'emphemeres. *C.R. Acad. Sci.* 150, 411–419.
- MOLLENHAUER, H. H. 1964. Plastic embedding mixtures for use in electron microscopy. *Stain Technol.*, 39, 111–114.
- SPRAGUE, V. 1977. "Systematics of the Microsporidia." Plenum, New York.
- VENABLE, J. H., AND COGGESHALL, R. 1965. A simplified lead citrate stain for use in electron microscopy. *J. Cell Biol.*, 25, 407–408.
- WEISER, J. 1961. Die Mikrosporidien als Parasiten der Insekten. *Monogr. Angew. Entomol.*, 17, 1–149.